https://doi.org/10.5194/egusphere-2026-1812
Preprint. Discussion started: 20 April 2026

Precipitation variability inferred from tree rings in the eastern Tianshan Mountains over the past two centuries

Maierdang Keyimu[1,2*], Xiaofei Ma[1], Zongshan Li[3], Ze-xin Fan[4], Yesi Zhao[5], Fanjiang Zeng[1,2]

1. State Key Laboratory of Ecological Safety and Sustainable Development in Arid Lands, Xinjiang Institute of Ecology and Geography, Chinese Academy of Sciences, Urumqi 830011, Xinjiang, China
2. Cele National station of Observation and Research for Desert-Grassland Ecosystems, Cele 848300, Xinjiang, China
3. State Key Laboratory of Urban and Regional Ecology, Research Center for Eco-Environmental Sciences, Chinese Academy of Sciences, Beijing 100085, China
4. CAS Key Laboratory of Tropical Forest Ecology, Xishuangbanna Tropical Botanical Garden, Chinese Academy of Sciences, Mengla 666303, China
5. Laboratory for Climate Risk and Urban-Rural Smart Governance, School of Geography, Jiangsu Second Normal University, Nanjing 210013, China

*Corresponding author: Maierdang Keyimu (mhk@ms.xjb.ac.cn).

https://doi.org/10.5194/egusphere-2026-1812
Preprint. Discussion started: 20 April 2026

Abstract: Tree rings serve as precise archives of the environmental conditions that influence tree growth. In this study, we collected tree-ring cores from Schrenk spruce (*Picea schrenkiana*) in the eastern Tianshan Mountains and developed a robust ring-width chronology. Growth-climate response analysis revealed that total precipitation from the previous July through the current June is the primary factor limiting radial growth in this species, a relationship that remained stable over the period 1961–2020. Based on this strong climatic signal, we reconstructed annual precipitation for the region from 1830 to 2020. The reconstruction explains 37.6% of the variance in instrumental precipitation records, demonstrating its reliability as a proxy for past climate. The reconstructed series identified distinct dry periods (e.g., 1830–1839, 1863–1868, 1919–1921, 1944–1947, 1975–1979, and 1989–1992) and wet periods (e.g., 1844–1850, 1869–1882, 1886–1899, 1930–1942, 1966–1973, 1980–1988, 1996–2001, and 2004–2018). The validity of our reconstruction is further supported by its strong agreement with other precipitation and drought reconstructions from nearby regions. Moreover, comparison with the Climatic Research Unit (CRU) gridded dataset indicates that our reconstruction captures precipitation variability across a broad spatial domain. By extending the instrumental record, this long-term precipitation series significantly enhances our understanding of climatic variability and its spatiotemporal characteristics in the eastern Tianshan Mountains. Notably, the reconstruction reveals a general upward trend in annual precipitation since the 1990s, which may enhance growth and carbon sequestration potential of Schrenk spruce forests in the region.

Keywords: Tree rings; Tianshan Mountain; Schrenk spruce; Precipitation reconstruction

https://doi.org/10.5194/egusphere-2026-1812
Preprint. Discussion started: 20 April 2026

Introduction

The Tianshan Mountains constitute one of Central Asia's most significant mountain systems, stretching approximately 2,500 km along an east–west axis and covering an area of roughly 800,000 km². This extensive range traverses multiple national borders, extending from Uzbekistan and Kyrgyzstan in the west, through southeastern Kazakhstan, and into China's Xinjiang region (Xiao et al., 2004, 2013, 2015). By virtue of its immense scale and central location, the Tianshan serves as a critical geographical and climatic divide within the Eurasian continent.

A fundamental hydroclimatic gradient exists along the Tianshan Mountains, driven primarily by differential moisture availability (Sun et al., 2012; Guan et al., 2022). The western sector lies under the dominant influence of the mid-latitude westerlies, which transport moisture from the Atlantic Ocean, the Mediterranean, and western Asia (Li et al., 2025). In contrast, the eastern Tianshan is situated deep within the continental interior, far removed from these primary moisture sources. Although limited moisture may occasionally arrive from distant sources such as the Arctic Ocean or via monsoonal incursions, its transport across vast arid landscapes results in substantial precipitation depletion. Therefore, reconstructing the long-term hydroclimatic history of the eastern Tianshan using extended proxy chronologies is of paramount importance for deciphering past climatic phases and understanding environmental shifts within this ecologically fragile region.

Dendroclimatology, which focuses on reconstructing past climate conditions from tree-ring data, is a fundamental approach for investigating pre-instrumental climate variability (Fritts, 1976). Tree rings serve as an exceptionally valuable proxy archive due to their annual resolution, absolute dating control, broad spatial coverage, and direct physiological sensitivity to environmental variables such as temperature and moisture availability (Yuan et al., 1994; Gou et al., 2006). These attributes enable the development of robust, precisely dated chronologies that can extend over centuries (Keyimu et al., 2021a,b). Consequently, tree-ring records play a pivotal role in reconstructing historical environmental and climatic changes across regional, hemispheric, and global scales, particularly over the past several centuries and beyond (Zhang et al., 2003; Liu et al., 2009; Yang et al., 2014). By quantifying past climate variability, dendroclimatological studies provide critical insights into the range, frequency, and magnitude of natural climatic oscillations. This knowledge not only advances our understanding of the mechanisms driving the climate system but also establishes

https://doi.org/10.5194/egusphere-2026-1812
Preprint. Discussion started: 20 April 2026

essential baselines for assessing contemporary anthropogenic climate change. Ultimately, tree-ring reconstructions offer invaluable long-term context that enhances the accuracy of climate models and refines projections of future climate trends.

Schrenk spruce (*Picea schrenkiana*) is a long-lived, widely distributed conifer that dominates forest ecosystems in the eastern Tianshan Mountains. Owing to its climatic sensitivity, longevity, and extensive geographical range, this species serves as an exceptional archive for dendroclimatological research. Consequently, it has been widely employed both for reconstructing past climate variability (Yuan et al., 2003; Chen et al., 2008; Shang et al., 2010; Zhang et al., 2015; Chen et al., 2016; Zhang et al., 2017; Jiang et al., 2017; Gou et al., 2023; Ma et al., 2025) and for assessing how climatic variability influences the composition, productivity, and functional dynamics of montane ecosystems. Although a substantial body of dendroclimatological research in the Tianshan Mountains has successfully reconstructed historical hydroclimatic variability, these studies have predominantly focused on drought indices and aridity patterns. In contrast, high-resolution reconstructions of precipitation variability remain relatively scarce. This research gap is significant, as direct precipitation reconstructions are essential for understanding the region's full water cycle dynamics, ecological responses, and long-term hydroclimatic trends—perspectives that extend beyond the scope of drought metrics alone.

In this study, we collected tree-ring samples from Schrenk spruce in Mulei County, located in the eastern Tianshan Mountains. Our primary objectives were to: (1) develop a robust tree-ring width chronology and identify the climatic drivers of radial growth; (2) reconstruct historical hydroclimatic variability and contextualize recent changes within a multi-century framework; and (3) evaluate the fidelity of the reconstruction using statistical and comparative approaches. Our findings not only enhance the existing network of hydroclimatic records in the eastern Tianshan Mountains but also provide a valuable long-term baseline for assessing contemporary precipitation trends. Furthermore, this reconstruction offers critical insights for evaluating the future trajectory and resilience of regional forest ecosystems under changing climatic conditions.

Materials and methods

Sampling sites

Tree-ring samples were collected from Schrenk spruce trees in Dongcheng Village, Mulei County,

https://doi.org/10.5194/egusphere-2026-1812
Preprint. Discussion started: 20 April 2026

located in the eastern Tianshan Mountains (Fig. 1). The region experiences a temperate continental climate characterized by semi-arid conditions. Meteorological data from the Mulei station (1960–2020) indicate a mean annual temperature of 5.4°C, with monthly means ranging from –32.1°C in January to 37.9°C in July. Mean annual precipitation totals 330 mm, more than 80% of which falls between April and September (Fig. 2). To maximize the climatic signal in the tree-ring series (Li et al., 2017), cores were extracted from healthy, spatially isolated trees across five sampling sites at an elevation of approximately 2300 m a.s.l. A single core was collected from each of 180 trees using a 5.1 mm increment borer. Sampling was oriented perpendicular to the slope to minimize the influence of tension wood (Keyimu et al., 2021).

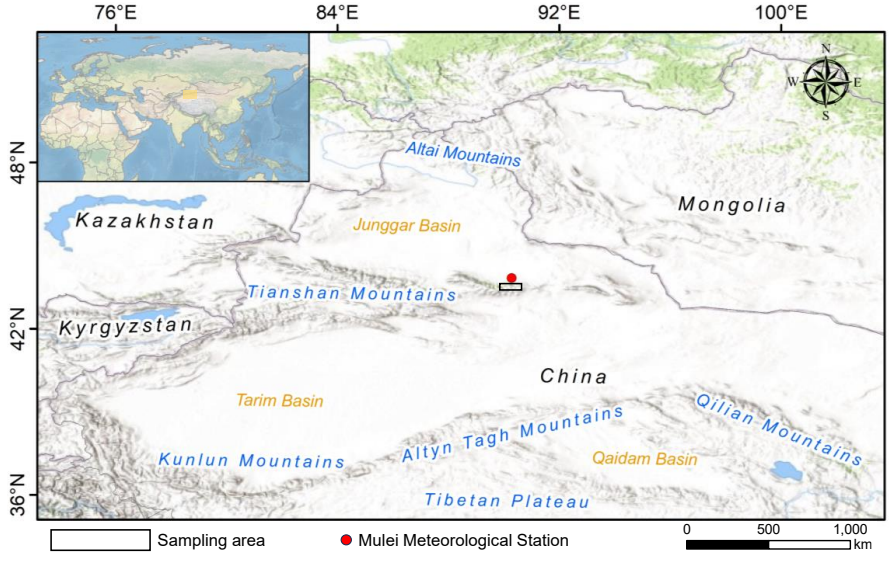

Fig. 1 Location map of the study region showing the tree ring sampling area and the meteorological station.

Tree ring measurement and establishment of chronology

Collected tree-ring samples were processed following standardized dendrochronological procedures to ensure data quality and comparability. Cores were first secured onto wooden mounts, air-dried, and progressively sanded with 360, 600, and 1000 grit sandpaper to achieve a flat, polished surface with clearly visible ring boundaries. The prepared samples were then scanned using a TSD4800 flatbed scanner, and ring widths were measured from the digital images at 0.001 mm resolution using the WinDENDRO 2017a system (Keyimu et al., 2025). Cross-dating was performed by

https://doi.org/10.5194/egusphere-2026-1812
Preprint. Discussion started: 20 April 2026

marking decadal intervals and visually matching growth patterns among samples; dating quality was subsequently verified using the COFFECHA program (Holmes, 1983). After excluding poor-quality or undateable cores, 161 series were retained for final analysis. To remove age-related growth trends, each series was detrended using a negative exponential curve (Cook et al., 1995) implemented in the dplR package (Bunn, 2018) of R program. A standard tree-ring width (TRW) chronology was then developed. Several standard dendrochronological statistics were computed to evaluate chronology quality. Common signal strength among measurement series was assessed using mean inter-series correlation (Rbar), signal-to-noise ratio (SNR), and variance of the first eigenvector (VFE). Inter-annual variability was characterized by standard deviation (SD) and mean sensitivity (MS). Finally, the expressed population signal (EPS), with a threshold of >0.85, was applied to determine the reliably expressed portion of the chronology (Wigley et al., 1984).

Climate data

Climate data for growth–climate relationship analyses and reconstruction calibration were obtained from the Mulei Meteorological Station, located near the sampling area. Monthly records of maximum, minimum, and mean temperature (Tmax, Tmin, Tmean), as well as total precipitation (Pre), covering the period 1960–2020, were acquired from the China Meteorological Data Sharing Service System. Self-calibrating Palmer Drought Severity Index (scPDSI) data for the same interval were sourced from the Climatic Research Unit (CRU) TS 4.07 dataset via the KNMI Climate Explorer interface (accessed 20 November 2025).

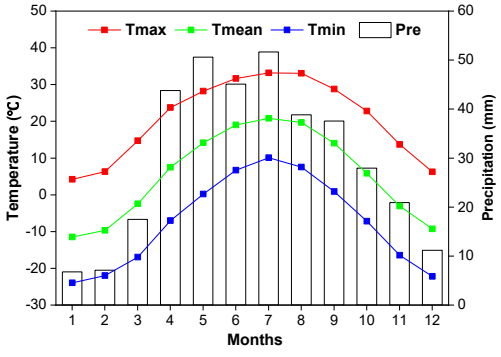

Fig. 2 Monthly instrumental data for temperature and precipitation obtained from the Mulei station, spanning the years 1960 through 2020.

Growth – climate relationship analysis

https://doi.org/10.5194/egusphere-2026-1812
Preprint. Discussion started: 20 April 2026

Response and correlation function analyses between tree-ring indices and monthly climate data were conducted using the DENDROCLIM2002 software (Biondi and Waikul, 2004). Correlations between the TRW chronology and climate variables were evaluated over the common period 1960–2020. To account for the carryover effect of prior-year climate conditions on current-year growth (Fritts, 1976), the analysis incorporated a 16-month temporal window extending from the previous June to the current September. Seasonalized climate variables were also examined, as they provide a more ecologically meaningful timescale for growth than do individual months. The temporal stability of climate–growth relationships was assessed using a 30-year moving correlation window. For all analyses, correlations were considered statistically significant at the 95% confidence level.

Establishment of reconstruction model and its evaluation

A linear regression model for climate reconstruction was developed based on the established relationship between tree-ring growth and the primary climatic limiting factor (Cook and Kairiukstis, 1990). Model fidelity was assessed using a split-sample calibration-verification approach, following standard dendroclimatological practice. Model performance was evaluated using a suite of statistics, including Pearson's correlation coefficient (r), explained variance (R^2), adjusted explained variance (R^2_{adj}), reduction of error (RE), coefficient of efficiency (CE), and the sign test (ST) (Fritts et al., 1990).

Results

Characteristics of tree – ring width chronology

The key descriptive metrics of the standard tree-ring width chronology (Fig. 3) are summarized in Table 1. A strong common signal among trees is indicated by a mean interseries correlation (Rbar) of 0.53 and a variance in the first eigenvector (VFE) of 31.11%. These statistical characteristics demonstrate the chronology's suitability as a reliable proxy for investigating climatic variability in the eastern Tianshan Mountains. The chronology exhibits moderate year-to-year variability, with a mean sensitivity (MS) of 0.20 and a standard deviation (SD) of 0.29. A first-order autocorrelation (AC1) of 0.69 indicates a significant carryover effect of growing conditions from previous years. The high signal-to-noise ratio (SNR) further supports the presence of a strong common climatic signal in the radial growth of the sampled trees. Based on a running expressed population signal (EPS) threshold of >0.85, the reliably expressed portion of the chronology spans 191 years, from

https://doi.org/10.5194/egusphere-2026-1812
Preprint. Discussion started: 20 April 2026

1830 to 2020.

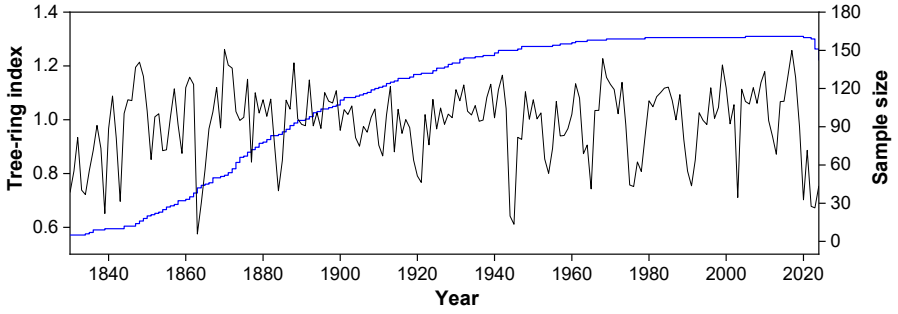

Fig. 3 Standard TRW chronology and sample size for Schrenk spruce in the eastern Tianshan Mountains (chronology: black line; sample size: blue line).

Table 1 Site information, chronology statistics and results of a common interval span analysis of standard tree-ring width (TRW) chronology from the eastern Tianshan Mountains, China

Data type	Time length	Number of cores	SD	MS	Rbar	SNR	EPS	VFE
Tree ring width	1830-2020	161	0.14	0.27	0.46	36.20	0.97	0.48

Tree growth and climate relationship analyses

Correlations between the TRW chronology and monthly climate variables over the 1961–2020 period are presented in Fig. 3. The analysis reveals a consistent pattern: radial growth exhibits positive correlations with hydroclimatic factors (precipitation and scPDSI) across most monthly windows, while demonstrating consistently negative correlations with all three temperature variables (Tmax, Tmin, Tmean). This pattern—whereby moisture availability favors growth and temperature exerts a limiting influence—is further supported by correlations using aggregated monthly climate data (Supplementary File). Among all climatic variables examined, total precipitation from the previous July through the current June showed the strongest association with radial growth, yielding a correlation coefficient of 0.62 ($p < 0.01$). Accordingly, annual precipitation was selected as the target variable for climate reconstruction in this study.

https://doi.org/10.5194/egusphere-2026-1812
Preprint. Discussion started: 20 April 2026

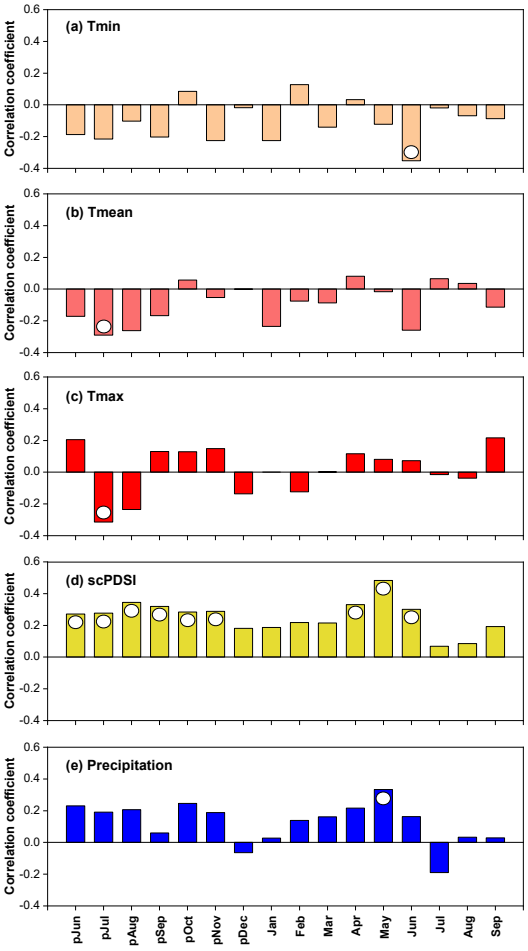

185

186 **Fig. 4** Correlations of tree-ring width with temperature, precipitation, and scPDSI over the climatic
187 window spanning from June of the previous year to September of the current year for the common
188 period from 1961 to 2020. The while circle indicates the correlations reaching 95% significant level.

https://doi.org/10.5194/egusphere-2026-1812
Preprint. Discussion started: 20 April 2026

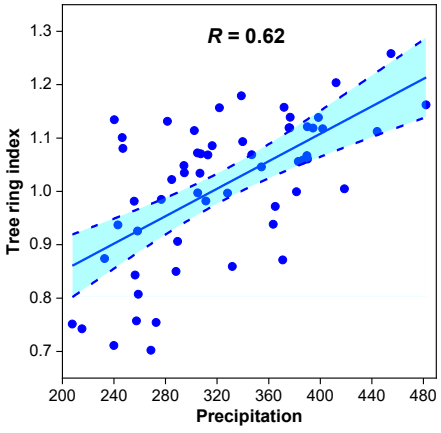

Fig. 5 Correlation between tree-ring width and July–June precipitation during the period of 1961–2020. The correlation is significant at 99% level.

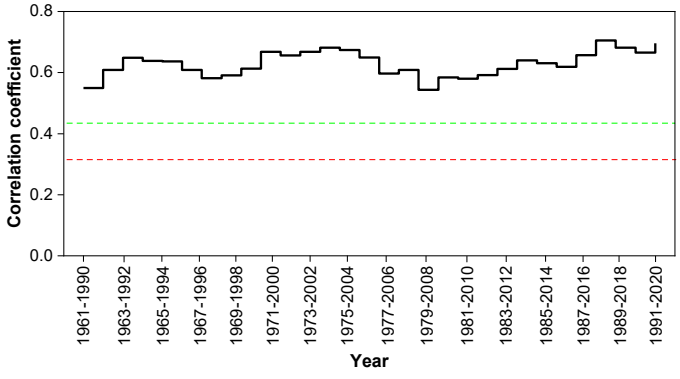

Fig. 6 The moving correlation between the TRW chronology and annual precipitation over the period 1961–2020. The horizontal red and dashed green lines represent the 0.05 and 0.01 significance levels, respectively.

Annual precipitation reconstruction

Based on the established relationship between tree growth and precipitation, a linear regression model was developed to reconstruct annual precipitation from 1830 to 2020: Annual precipitation (mm) = 296.28 × TRW index + 25.53. The reconstruction accounts for 37.6% of the variance in observed precipitation during the instrumental period (1961–2020). Close agreement between reconstructed and instrumental series is visually evident in Fig. 7. A split-sample calibration-verification procedure was employed to rigorously evaluate reconstruction reliability (Table 2).

https://doi.org/10.5194/egusphere-2026-1812
Preprint. Discussion started: 20 April 2026

Positive values for the reduction of error (RE = 0.18) and coefficient of efficiency (CE = 0.15) demonstrate the model's predictive skill and reconstruction robustness. Model performance is further confirmed by a significant sign test ($p < 0.05$), validating the reconstruction's ability to capture inter-annual variability, and by a significant F-test ($p < 0.01$). Collectively, these statistics confirm that the reconstruction model is valid and possesses reliable predictive capability for estimating historical precipitation in the study region.

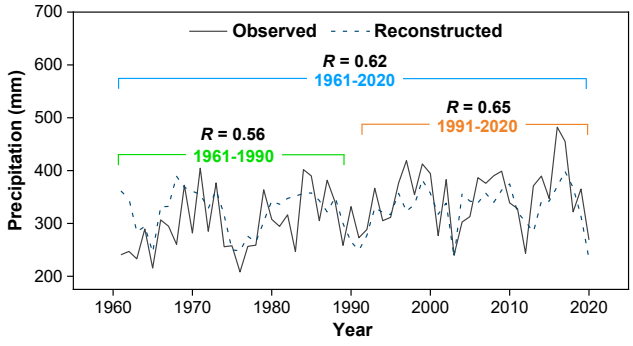

Fig. 7 Observed (black continuous line) and model-reconstructed (black dotted line) annual precipitation from 1961 to 2020. The correlations between the periods of 1961-1990, 1990-2020, and 1961-2020 are all significant at 99% level.

Table 2 Calibration and verification statistics for the precipitation reconstruction model (split-sample method)

Period	*r*	R^2	*F*	*RE*	*CE*	*S*
Calibration (1961-1990)	0.56	0.314	18.5	0.43	0.38	27+/11-
Verification (1991-2020)	0.65	0.423	19.0	0.49	0.42	30+/7
Full calibration (1961-2020)	0.62	0.382	25.3	—	—	—

Variability of historical annual precipitation

The annual precipitation reconstruction for 1830–2020 is presented in Fig. 8. The reconstructed series has a mean of 319.8 mm and a standard deviation (SD) of 39.4 mm. Based on these statistics, years were classified as wet (>359 mm, mean + 1SD) or extremely wet (>398 mm, mean + 2SD), and as dry (<280 mm, mean – 1SD) or extremely dry (<240 mm, mean – 2SD). A complete listing of these years is provided in Table 3. The reconstruction exhibits broad synchrony with previously documented dry/wet periods and extreme climate events from nearby hydroclimatic reconstructions

https://doi.org/10.5194/egusphere-2026-1812
Preprint. Discussion started: 20 April 2026

(Fig. 9), although some discrepancies are evident. Spatial correlation analyses (Fig. 10) indicate that both the instrumental and reconstructed precipitation series capture climatic variability across a similar geographical domain in the eastern Tianshan Mountains, demonstrating comparable spatial representativeness.

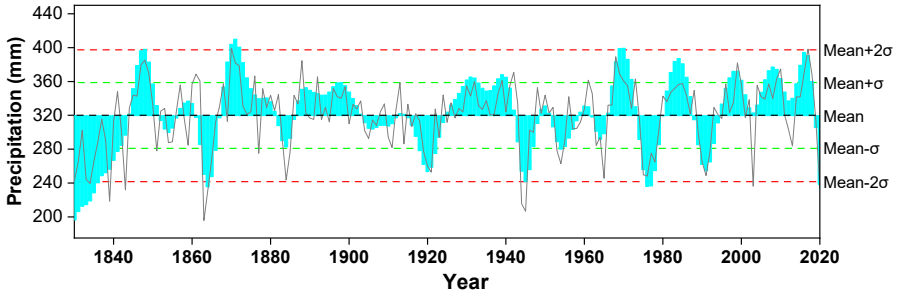

Fig. 8 Annual precipitation reconstruction for the eastern Tianshan Mountains. The gray line represents the annual reconstruction series, while the cyan shading denotes the 11-year loess-smoothed trend. A horizontal dashed black line indicates the long-term mean precipitation. Thresholds for classifying dry/extremely dry and wet/extremely wet years are shown by horizontal green and red dashed lines, respectively.

Table 3 Major dry and wet periods in the eastern Tianshan Mountains

Periods	Dry	Periods	Wet
	Average precipitation (mm)		Average precipitation (mm)
1830-1839	267.1	1844-1850	354.4
1863-1868	230.8	1869-1882	342.8
1883-1885	270.9	1886-1899	337.6
1919-1921	263.3	1930-1942	342.5
1944-1947	256.2	1966-1973	353.6
1953-1955	277.1	1980-1988	345.1
1975-1979	268.3	1996-2001	345.3
1989-1992	272.8	2004-2018	346.6

https://doi.org/10.5194/egusphere-2026-1812
Preprint. Discussion started: 20 April 2026

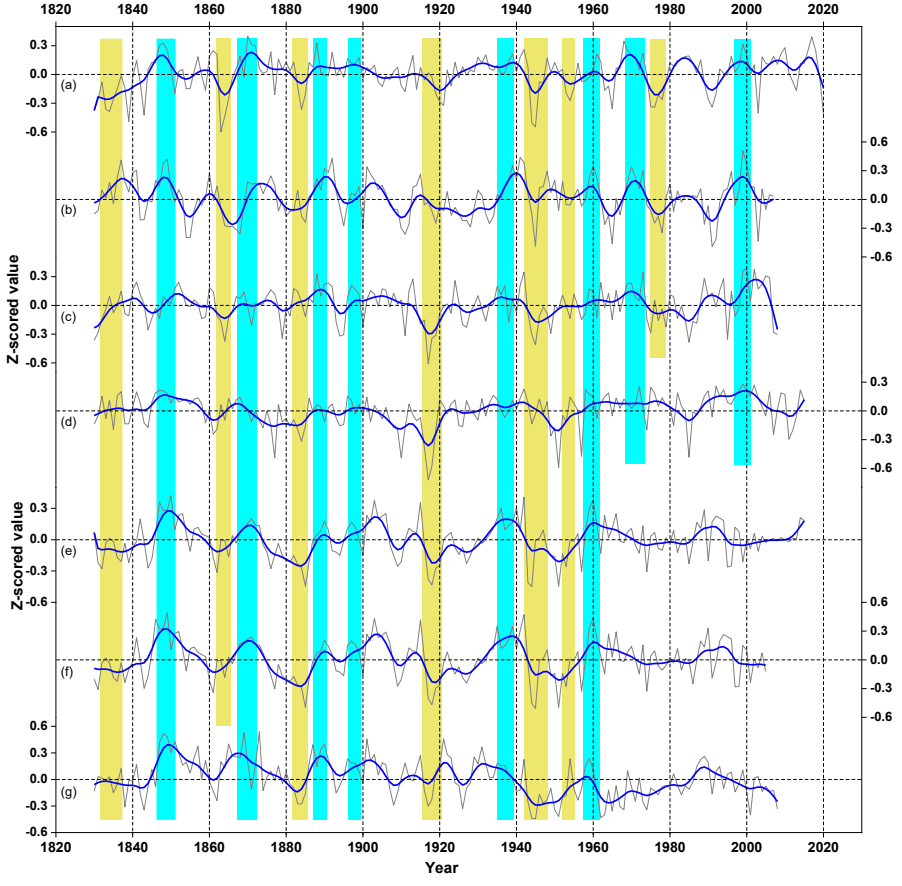

Fig. 9 Comparison of multiple hydroclimatic reconstructions across the Tianshan Mountains from different studies: (a) precipitation reconstruction from this study; (b) precipitation reconstruction for the eastern Tianshan Mountains (Zhang et al., 2015); (c) PDSI drought reconstruction for the inner Tianshan Mountains (Zhang et al., 2017); (d) SPEI drought reconstruction for the central Tianshan Mountains (Ma et al., 2025); (e) PDSI drought reconstruction for the Tianshan Mountains (Wang et al., 2021); (f) SPEI drought reconstruction for the central Tianshan Mountains (Jiang et al., 2017); and (g) SPEI drought reconstruction for the central Tianshan Mountains (Xu et al., 2014).

https://doi.org/10.5194/egusphere-2026-1812
Preprint. Discussion started: 20 April 2026

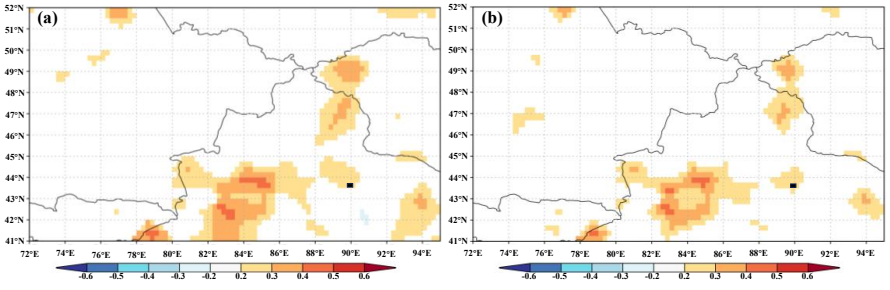

Fig. 10 Spatial correlations of actual (a) and reconstructed (b) precipitation with a gridded precipitation dataset during their overlapping periods (1961–2020). The black square indicates the location of the study site.

Discussion

Relationship between tree growth and climate

Moisture availability was identified as the primary factor limiting radial growth of Schrenk spruce in the eastern Tianshan Mountains. Correlation analysis revealed that total precipitation from the previous July to the current June exerted a stronger influence on growth than any other climate variable or seasonal window examined. This dominant role of precipitation was further corroborated by response function analysis. A 30-year moving correlation analysis (Fig. 6) demonstrated that the positive association between annual precipitation and tree growth has remained both temporally stable and statistically significant. This persistent relationship underscores the consistent and limiting role of moisture availability on forest productivity in this region.

In water-limited regions, precipitation exerts a critical influence on tree growth. This influence exhibits pronounced seasonal heterogeneity (Trouet et al., 2006), as moisture delivered during different times of the year serves distinct physiological functions within the annual growth cycle. The relative importance of precipitation varies substantially by season, ecosystem, and tree species (Parton et al., 2012). Spring precipitation is particularly critical for tree growth, especially in temperate, boreal, and arid regions, as it directly governs the physiological processes that initiate the annual growth cycle. This seasonal importance can be attributed to several key mechanisms.

Spring moisture availability governs the resumption of tree growth through several interrelated mechanisms. First, it ends winter dormancy by rehydrating tissues and enabling the reactivation of the vascular cambium—the cell division responsible for wood formation (cambial reactivation).

https://doi.org/10.5194/egusphere-2026-1812
Preprint. Discussion started: 20 April 2026

This moisture-dependent process promotes the expansion of newly formed, large-diameter tracheids that comprise the earlywood, the lighter, less dense portion of the annual ring (Rathgeber et al., 2017). Earlywood formation is particularly sensitive to water availability during spring. Concurrently, spring precipitation supports budbreak, leaf or needle emergence, and the development of the photosynthetic canopy (Die et al., 2017). By enabling the rapid establishment of a functional canopy, adequate spring moisture maximizes the growing season length and photosynthetic capacity. Consequently, insufficient spring precipitation can delay or severely curtail this initial growth phase, directly reducing the width of the annual ring.

Summer precipitation plays a critical role in sustaining active tree growth and preventing drought stress. It supports photosynthesis by maintaining leaf turgor and keeping stomata open for CO_2 uptake (John and Boyer, 2015). Additionally, summer precipitation replenishes soil moisture lost to evapotranspiration, thereby enabling continued cell wall thickening during latewood formation (Antonova et al., 2014) and preventing the premature shutdown of growth processes. Conversely, summer drought induces stomatal closure, halting photosynthesis and potentially leading to carbon starvation. Severe water deficit can also cause cell collapse, resulting in the formation of dense, narrow latewood bands or, in extreme cases, missing rings (Novak et al., 2011).

Consistent with dendroclimatological theory (Fritts, 1976), our analyses revealed a significant time-lag effect: precipitation during the preceding autumn and winter exhibited a pronounced carry-over influence on tree-ring growth in the following year. This persistence is further supported by the relatively high first-order autocorrelation (AR1 = 0.68) of the TRW chronology in present study. Specifically, correlations between tree growth and climate variables demonstrated that precipitation during the previous autumn strongly influenced current-year radial growth of Schrenk spruce. This lagged effect can be attributed to several vital physiological and ecological functions of autumn precipitation. Beyond sustaining late-season growth, autumn precipitation critically recharges soil moisture—particularly in deeper soil layers—following summer depletion (Wagner et al., 2015). This replenishment aids nutrient uptake for energy storage and supports continued root growth before winter dormancy (Li et al., 2024). Collectively, these processes create a crucial hydrological reserve that trees can draw upon during growth initiation the following spring. Conversely, a dry autumn leads to depleted soil moisture reserves entering winter, predisposing trees to spring drought

https://doi.org/10.5194/egusphere-2026-1812
Preprint. Discussion started: 20 April 2026

stress (Bohnhorst et al., 2025). This vulnerability is particularly pronounced in regions such as our study area, where spring precipitation is limited.

In the eastern Tianshan Mountains, winter precipitation falls primarily as snow. The resulting snowpack acts as an insulating layer, maintaining unfrozen soil conditions beneath and allowing soil processes to continue, albeit at reduced rates (Edwards, 2007). This protection is critical for conifer roots, as unfrozen soil buffers shallow root systems against freezing temperatures (Schenk and Jackson, 2002), thereby reducing the metabolic energy required for repair and regeneration in the following spring (Pederson et al., 2004). The conserved energy can instead be allocated to initiate xylogenesis and form earlywood cells at the start of the growing season. Furthermore, for evergreen species such as Schrenk spruce, which maintain low levels of photosynthetic activity year-round (Prats and Brodersen, 2020), moisture available from the snowpack and unfrozen soil supports continued carbohydrate accumulation even during winter. This process enhances the tree's energy reserves prior to the spring growth flush. In contrast, radial tree growth exhibited negative or insignificant correlations with temperature across most monthly windows (Fig. 4). This pattern can be explained by the fact that higher temperatures enhance evapotranspiration, thereby reducing available soil moisture and ultimately constraining tree growth in this water-limited environment.

Validity of the historical climate reconstruction

The reconstructed precipitation series reveals clear alternating episodes of dry and wet conditions (Fig. 8). To evaluate the reliability and spatial coherence of our reconstruction, we compared it with other hydroclimatic reconstructions from surrounding regions. For improved visual clarity in this comparison, an 11-year loess smoothing function was applied to each dataset (Fig. 9). The reconstructed hydroclimatic series exhibits general agreement with prior studies regarding the timing of major dry and wet periods. However, variations are evident in their specific temporal extent and magnitude. Correlation strength between our reconstruction and comparable records from surrounding regions (Zhang et al., 2015; Jiang et al., 2017; Zhang et al., 2017; Ma et al., 2017; Wang et al., 2021; Xu et al., 2014) is not uniform. These differential correlations may be partially explained by geographical proximity between study sites. Furthermore, discrepancies in reconstructed hydroclimatic signals can be attributed to several methodological differences, including the type of hydroclimatic variable reconstructed (e.g., precipitation, PDSI, SPEI), the

https://doi.org/10.5194/egusphere-2026-1812
Preprint. Discussion started: 20 April 2026

temporal focus of the reconstruction (annual, seasonal, or monthly), tree species used (which vary in drought tolerance and climatic sensitivity), the specific tree-ring parameter measured (e.g., total width, earlywood width, or density), chronology standardization method (standard vs. residual chronologies), length of the calibration period, sample depth, and geomorphological characteristics of sampling sites (e.g., elevation, slope aspect).

In order to validate the reconstructed wet and dry periods, we consulted historical archives documenting climatic extremes in the eastern Tianshan Mountains. These archival sources provide independent qualitative evidence that corroborates our tree-ring-based precipitation reconstruction. For instance, compiled historical accounts document a severe spring drought in eastern Northwest China during 1867, which critically reduced agricultural output. Over 80% of sown farmland failed to produce a harvest, leading to severe famine (The Complete Collection of Qing Dynasty Chronicles, 2006). Historical records further identify a major, widespread drought beginning in the 1910s and persisting into the 1920s across the study region and wider Tianshan area (Li et al., 2014). Reconstructions concur that this event affected eastern, central, and western Tianshan, with devastating socio-ecological consequences across Central Asia, including pasture degradation, widespread livestock mortality, and acute food shortages (Xiang et al., 1994). The scale of impact was catastrophic: livestock numbers in Uzbekistan reportedly declined from approximately 9 million in 1900 to only 3 million by 1920, while famine claimed an estimated 1.4 million lives in western Kazakhstan in 1920 alone (Aberhor et al., 1998). Another particularly severe drought occurred in 1945, affecting the entire Tianshan region and Central Asia. In northwest China's Shaanxi-Gansu area, this drought impacted over 500,000 hectares of cropland, reducing grain yields by more than 40% (Zhai and Peng, 2009). Climatic analysis links this extreme event to a La Niña (cold-phase ENSO) episode and cooler sea surface temperatures in the Arabian Sea and northern Indian Ocean (Wang et al., 2008). This oceanic configuration altered atmospheric circulation patterns, severely reducing moisture transport to Central Asia (Li et al., 2010). The resulting aridity is strongly corroborated by proxy data: moisture-sensitive tree-ring records across the region exhibit exceptionally narrow growth rings for 1945, providing independent evidence of profoundly dry conditions.

The wet periods identified in our climate reconstruction correspond closely with documented major

https://doi.org/10.5194/egusphere-2026-1812
Preprint. Discussion started: 20 April 2026

flood events in historical records. For instance, the 1890s were characterized by relatively humid conditions across the Tianshan Mountains. This climatic pattern manifested in extreme weather events, such as an intense precipitation episode in the eastern Tianshan region in 1891, which triggered severe flooding that devastated the entire Balikun area (Wen et al., 2006). The central Tianshan Mountains were similarly affected: persistent precipitation in 1892 resulted in catastrophic flooding that obliterated the Kuitun area, causing widespread inundation that crippled transportation networks and damaged infrastructure. This pattern of climatic-hydrological linkage continued into the wet period of the 1930s–1940s. Historical archives report that a major precipitation event in 1940 caused severe flooding in Hami, located in eastern Xinjiang. That same year, another episode of sustained heavy rainfall led to significant flooding in both Hami and the Changji area (Wen et al., 2006). Concurrently, the Urumqi River overflowed due to extreme rainfall, inflicting extensive damage throughout the city of Urumqi. These recurrent disasters across different decades and sub-regions consistently demonstrate the strong association between extended wet phases in our reconstruction and the occurrence of historically significant floods, providing independent validation of our precipitation reconstruction.

To assess the spatial representativeness of our precipitation reconstruction, we performed a spatial correlation analysis against gridded climate data. Both the instrumental records and our reconstructed series for the common period 1961–2020 were uploaded to the KNMI Climate Explorer platform for consistent processing. Using this platform, we computed spatial correlation fields between our datasets and gridded precipitation data from the Climatic Research Unit (CRU). The analysis revealed similar spatial correlation patterns between the instrumental data and our reconstruction. This consistent spatial footprint demonstrates that our reconstruction reliably captures regional-scale precipitation variability. Therefore, the reconstruction can be considered a robust proxy for representing historical hydroclimatic conditions across a broad area of the eastern Tianshan Mountains.

Conclusion

In this study, we developed a tree-ring width (TRW) chronology from Schrenk spruce (*Picea schrenkiana*) sampled in the eastern Tianshan Mountains, northwestern China. Climate–growth analysis revealed that radial growth of Schrenk spruce in this region is primarily limited by moisture

https://doi.org/10.5194/egusphere-2026-1812
Preprint. Discussion started: 20 April 2026

availability. Based on this relationship, we reconstructed historical precipitation variability using a linear regression model that explains 37.6% of the variance in observed precipitation. Our reconstruction identifies several major hydroclimatic phases over the past two centuries. Notable dry periods occurred during 1830–1839, 1863–1865, 1883–1885, 1919–1921, 1944–1947, 1953–1955, 1975–1979, and 1989–1992. Pronounced wet intervals were detected in 1844–1850, 1868–1882, 1886–1899, 1930–1942, 1966–1973, 1980–1988, 1996–2001, and 2004–2018. The reconstruction demonstrates strong spatial coherence with other hydroclimate records from the Tianshan region. Moreover, the timing of major dry and wet phases corresponds closely with historically documented droughts and flood events, providing independent validation of our precipitation reconstruction. By extending the instrumental climate record, this study provides a long-term perspective on precipitation variability in the eastern Tianshan Mountains and contributes to a more comprehensive understanding of regional hydroclimatic dynamics.

Our results reveal a general increase in annual precipitation since the 1990s, a trend that has supported forest ecosystem development in the region. This hydroclimatic shift is favorable for enhancing the carbon sequestration capacity of moisture-sensitive tree species in the eastern Tianshan Mountains. Future research should prioritize expanding the spatial coverage of tree-ring sampling networks and developing a more comprehensive array of long-term proxy chronologies. Such datasets are essential for reconstructing historical climate variability across longer timescales and broader spatial domains within the Tianshan Mountains, thereby deepening our understanding of past hydroclimatic dynamics and their ecological implications.

Acknowledgment

This work was funded by the Youth Innovation Promotion Association of Chinese Academy of Sciences (grant no. 2022445). We are grateful to the editor and anonymous reviewers for their valuable comments and suggestions to improve this article.

Funding declaration

This work was funded by the Youth Innovation Promotion Association of Chinese Academy of Sciences (grant no. 2022445)

Data availability statement

https://doi.org/10.5194/egusphere-2026-1812
Preprint. Discussion started: 20 April 2026

The data in this manuscript is available on reasonable request.

Author contribution statement

Conceptualization: Maierdang Keyimu and Zongshan Li; methodology: Maierdang Keyimu, Xiaofei Ma, Yesi Zhao; software: Maierdang Keyimu, Xiaofei Ma; validation: Zongshan Li, Maierdang Keyimu, Ze-xin Fan; formal analysis: Maierdang Keyimu; investigation: Maierdang Keyimu; resources: Fanjiang Zeng, Zongshan Li, and Xiaofei Ma; data curation: Ze-xin Fan and Yesi Zhao; writing—original draft preparation: Maierdang Keyimu; writing—review and editing: Zongshan Li and Ze-xin Fan; supervision: Maierdang Keyimu and Fanjiang Zeng; project administration: Maierdang Keyimu; funding acquisition: Maierdang Keyimu. All authors have read and agreed to the submitted version of the manuscript.

Declare of interest

The authors declare that they don't have conflict of interest.

References:

Abelkhozhin. Historical topics of Kazakhstan—a country in the heart of Eurasia. Almaty. 1998, p. 209.

Antonova, G.F., Varaksina, T.N., Zheleznichenko, T.V., Stasova, V.V. Lignin deposition during earlywood and latewood formation in Scots pine stems. Wood Science and Technology, 2014, 48(5), 919–936. https://doi.org/10.1007/s00226-014-0650-3

Biondi, F., Waikul, K. DENDROCLIM2002: a C++program for statistical calibration of climate signals in tree ring chronologies. Computer in Geoscience, 2004, 30, 303–311, https://doi.org/10.1016/j.cageo.2003.11.004.

Bohnhorst, L., Biber, P., Uhl, E., Pretzsch, H. Quantification of the drought stress response of trees depending on their past growth. Forest Ecology and Management, 555, 122064. https://doi.org/10.1016/j.foreco.2025.122064

Boyer, J.S. Turgor and the transport of CO_2 and water across the cuticle (epidermis) of leaves. Journal of Experimental Botany, 2015, 66(9), 2625–2633. https://doi.org/10.1093/jxb/erv065

Bunn, A.G. A dendrochronology program library in R (dplR). Dendrochronologia, 2008, 26(2): 115-

https://doi.org/10.5194/egusphere-2026-1812
Preprint. Discussion started: 20 April 2026

124. DOI:10.1016/j.dendro.2008.01.002.

Chen, F., Shang, H.M, Yuan, Y.J. Dry/wet variations in the eastern Tien Shan (China) since AD 1725 based on Schrenk spruce (*Picea schrenkiana* Fisch et Mey) tree rings. Dendrochronologia, 2016, 40, 110-116. https://dx.doi.org/10.1016/j.dendro.2016.07.003

Chen, X.J., Yuan, Y.J., Chen, F. Analysis of tree-ring width chronology characteristics from eastern area on north slope of Tianshan Mountains. Journal of Desert Research, 2008, 28(5), 833-841.

Cook, E.R. Kairiukstis, A. Methods of Dendrochronology: Applications in the Environmental Sciences, Kluwer Academic Press, Dordrecht, 1990, 406 pp.

Cook, E.R., Briffa, K.R., Meko, D.M., Graybill, D.A., Funkhouser, G. The 'segment length curse' in long tree-ring chronology development for palaeoclimatic studies. Holocene, 1995, 5, 229–237, https://doi.org/10.1177/095968369500500211.

Dié, A., Kitin, P., Kouamé, F. N., Van den Bulcke, J., Van Acker, J., & Beeckman, H. Fluctuations of cambial activity in relation to precipitation result in annual rings and intra-annual growth zones of xylem and phloem in teak (Tectona grandis) in Ivory Coast. IAWA Journal, 2012, 33(1), 3–15. https://doi.org/10.1163/22941932-90000078

Edwards, A.C., Scalenghe, R., Freppaz, M. Changes in the seasonal snow cover of alpine regions and its effect on soil processes: a review. Quaternary International, 2007, 162–163, 172–181, https://doi.org/10.1016/j.quaint.2006.10.027, 2007.

Fritts, H.C. Tree rings and climate, Academic Press, London, 1976, 582 pp., ISBN 978-0-1241-4212-1.

Fritts, H.C., Guiot, J., Gordon, G.A. Verification, in: Methods of Dendrochronology: Applications in the Environmental Sciences, edited by: Cook, E. and Kairiukstis, L. A., Kluwer Academic Publishers, Dordrecht, 1990, 178–184.

Gallinat, A.S., Primack, R.B., Wagner, D.L. Autumn, the neglected season in climate change research. Trends in Ecology & Evolution, 2015, 30(3), 169–176.https://doi.org/10.1016/j.tree.2015.01.004

https://doi.org/10.5194/egusphere-2026-1812
Preprint. Discussion started: 20 April 2026

Gou, X., Zhang, T., Yu, S., Liu, K., Zhang, R., Shang, H., Qin, L., Fan, Y., Jiang, S., Zhang, H., Guo, D. Climate response of *Picea schrenkiana* based on tree-ring width and maximum density. Dendrochronologia, 2023, 78, 126067. https://doi.org/10.1016/j.dendro.2023.126067

Gou, X.H., Yang, M.X., Peng, J.F. Maxum temperature reconstruction for Animaqing Mountains over past 830 years based on tree ring records. Quaternary Sciences, 2006, 26(6): 991-998.

Guan, X., Langhamer, L., Schneider, C. Lagrangian analysis of moisture sources of precipitation in the Tianshan Mountains, Central Asia. Earth and Space Science, 2022, 9.DOI:10.1029/2022EA002318.

Holmes, R. L. Computer-assisted quality control in tree-ring dating and measurement. Tree-ring Bulletin, 1983, 43, 69–75.

Jiang, P., Liu, H.Y., Wu, X.C. Tree-ring-based SPEI reconstruction in central Tianshan Mountains of China since A.D. 1820 and links to westerly circulation. International Journal of Climatology, 2017.DOI:10.1002/joc.4884.

Keyimu M, Qi Y, Peng J, Zeng, F.J. Growth of *Tamarix ramosissima* Ledeb. is benefitting from the recent climate change at the southern Tarim basin, northwest China. Dendrochronologia, 2025, 94, 126427. DOI:10.1016/j.dendro.2025.126427.

Keyimu, M., Li, Z.S., Liu, G.H., Fu, B.J., Fan, Z.X. Tree-ring based minimum temperature reconstruction on the southeastern Tibetan Plateau. Quaternary Science Review, 2021, 251, 106712, https://doi.org/10.1016/j.quascirev.2020.106712.

Li, B., Liang, Z., Yu, Z., Acharya, K. Evaluation of drought and wetness episodes in a cold region (Northeast China) since 1898 with different drought indices. Natural Hazards, 2014, 71(3), 2063–2085. https://doi.org/10.1007/s11069-013-0999-x

Li, J., Jin, Y., Zhao, Y., Au, T.F., Wang, Y., Chen, Z. The intra-annual rhythm of *Pinus sylvestris* growth-climate responses under a warming climate at its southern distribution limits. Agricultural and Forest Meteorology, 2024, 346, 109871. https://doi.org/10.1016/j.agrformet. 2023.109871

Li, J.B., Cook, E.R., Chen, F.H., Gou, X.H., D'Arrigo, R., Yuan, Y.J. An extreme drought event in the central Tien Shan area in the year 1945. Journal of Arid Environments, 2010, 74(10), 1225-1231.

https://doi.org/10.5194/egusphere-2026-1812
Preprint. Discussion started: 20 April 2026

Li, J.B., Shi, J.F., Zhang, D.D., Yang, B., Fang, K.Y., Yue, P.H. Moisture increase in response to high-altitude warming evidenced by tree-rings on the southeastern Tibetan Plateau. Climate Dynamics, 2017, 48, 649–660, https://doi.org/10.1007/s00382-016-3101-z.

Li, S.G. (Ed.). Yearbook of drought disasters in Shaanxi Province. Xi'an Map Publishing House, 1999.

Li, X.R., Li, L.P., Liu, Y.J. Synergistic effects of two oceans on interannual anomalies of winter precipitation in Xinjiang, China. Plateau Meteorology, 2025, 44(5). DOI: 10.7522/j.issn.1000-0534.2025.00016.

Ma, Y., Song, H., Liu, Y. Drought reconstructions over the past 552 years based on minimum earlywood density in central Tianshan Mountains. Palaeogeography, Palaeoclimatology, Palaeoecology, 2025, 667. DOI:10.1016/j.palaeo.2025.112853.

Novak, K., de Luis, M., Čufar, K., & Raventós, J. Frequency and variability of missing tree rings along the stems of *Pinus halepensis* and Pinus pinea from a semiarid site in SE Spain. Journal of Arid Environments, 2011, 75(5), 494–498. https://doi.org/10.1016/j.jaridenv.2010.12.005

Parton, W., Morgan, J., Smith, D. Impact of precipitation dynamics on net ecosystem productivity. Global Change Biology, 2012, 18(3), 915-927. DOI:10.1111/j.1365-2486.2011.02611.x.

Pederson, N., Cook, E. R., Jacoby, G. C., Peteet, D. M., and Griffin, K. L. The influence of winter temperatures on the annual radial growth of six northern range margin tree species. Dendrochronologia, 2004, 22, 7–29, https://doi.org/10.1016/j.dendro.2004.09.005.

Prats, K.A., Brodersen, C.R. Seasonal coordination of leaf hydraulics and gas exchange in a wintergreen fern. AoB Plants, 2020, 12, plaa048, https://doi.org/10.1093/aobpla/plaa048.

Rathgeber, C.B.K. Conifer tree-ring density inter-annual variability – anatomical, physiological and environmental determinants. New Phytologist, 2017, 216(3), 621–625. https://doi.org/10.1111/nph.14763

Schenk, H.J., Jackson, R.B. The global biogeography of roots. Ecological Monograph, 2002, 72, 311–328, https://doi.org/10.1890/0012-9615(2002)072[0311:TGBOR]2.0.CO;2.

https://doi.org/10.5194/egusphere-2026-1812
Preprint. Discussion started: 20 April 2026

Shang, H.M., Wei, W.S., Yuan, Y.J. The 150 year precipitation change recorded by tree ring in the central Tianshan Mountains. Arid Zone Research, 2010, 27(3): 443-444

Song, Q., Li, T., Dong, H. Regional differentiation in the variations of surface moisture index in north Tianshan Mountains in 1962-2009. Chinese Journal of Ecology, 2012, 31(6), 1508–1516. DOI:10.1007/s11783-011-0280-z.

Trouet, V, Coppin, P., Beeckman, H. Annual growth ring patterns in *Brachystegia spiciformis* reveal influence of precipitation on tree growth. Biotropica, 2006, 38(3), 375-382. https://doi.org/10.1111/j.1744-7429.2006.00155.x

Wang XD, Li RY. Analysis of drought disease in Shanxi Gansu Ningxia region since 1950s. Journal of Inner Mongolia Normal University, 2008, 37(4), 554-557.

Wang, J.S., Li, J.B., Chen, F.H. Variation of the dryness in the recent 200 a derived from tree ring width records in the eastern Tianshan Mountains. Journal of Glaciology and Geocryology, 2007, 29(2), 209-221.

Wang, T., Bao, A.M., Xu, W.Q., Yu, R.D., Zhang, Q.L., Jiang, L.L., Nzabarinda, V. Tree-ring-based assessments of drought variability during the past 400 years in the Tianshan mountains, arid Central Asia. Ecological Indicators, 2021, 126, 107702. https://doi.org/10.1016/j.ecolind.2021.107702.

Wen, K.G., Shi, Y.G., Ren, Y.G. The documents of Chinese Meteorological Disaster: Volume of Xinjiang. Beijing: Climate Meteorological Publishers, 2006, 4-35, 75-146.

Wigley, T.M., Briffa, K.R., Jones, P.D. On the average value of correlated time series, with applications in dendroclimatology and hydrometeorology. Journal of Climate and Applied Meteorology, 1984, 23, 201–213

Xiang, Q., Shi, Z., Liu, D. The Soviet Union and the Chinese Revolution (1917–1949). Central Compilation & Translation Press, 1994, p. 28.

Xiao, W.J., Qin, K.Z., Sun, S., et al. Paleozoic accretionary and collisional tectonics of the eastern Chinese Tianshan: implications for crustal growth of central Asia. EGS-AGU-EUG Joint Assembly, 2003.

https://doi.org/10.5194/egusphere-2026-1812
Preprint. Discussion started: 20 April 2026

542 Xiao, W.J., Windley, B.F., Allen, M.B. Paleozoic multiple accretionary and collisional tectonics of
543 the Chinese Tianshan orogenic collage. Gondwana Research, 2013, 23(4), 1316-
544 1341.DOI:10.1016/j.gr.2012.01.012.

545 Xiao, W.J., Windley, B.F., Shu, S., Li, J.L., Huang, B.C., Han, C.M., Yuan, C., Sun, M., Chen, H. A
546 tale of amalgamation of three permo-triassic collage systems in Central Asia: oroclines, sutures, and
547 terminal Accretion. Annual Review Earth and Planetary Sciences, 2015, 43, 477-507.
548 https://doi.org/10.1146/annurev-earth-060614-105254

549 Xu, G., Liu, X., Qin, D. et al. Drought history inferred from tree ring δ13C and δ18O in the central
550 Tianshan Mountains of China and linkage with the North Atlantic Oscillation. Theoretical and
551 Applied Climatology, 2014, 116, 385–401. https://doi.org/10.1007/s00704-013-0958-1

552 Yuan, Y., Li, J., Zhang, J. Variations of the spring precipitation day numbers reconstructed from tree
553 rings in the Urumqi River drainage, Tianshan Mts. over the last 370 years. Chinese Science Bulletin,
554 2003, 48(14), 1507–1510. https://doi.org/10.1360/03wd0110

555 Zhai, L., Feng, Q. Spatial and temporal pattern of precipitation and drought in Gansu Province,
556 Northwest China. Natural Hazards, 2008, 49(1).

557 Zhang, R.B., Yuan, Y.J., Yu, S.L., Chen, F., Zhang, T.W. Past changes of spring drought in the inner
558 Tianshan Mountains, China, as recorded by tree rings. Boreas, 2017, 46(4), 688–696.

559 Zhang, T.W., Yuan, Y.J., Chen, X.J. Tree ring width based precipitation for the Mulei Region in the
560 eastern Tienshan Mountains. Quaternary Sciences, 2015, 35(5): 1121-1133.